DOI: 10.13009/EUCASS2019-767

Thermal System Oriented Simulation of Aircraft Electrical Environmental Control Systems Including its Electric Coupling

Nicolás Ablanque, Santiago Torras*, Carles Oliet*, Joaquim Rigola* and Carlos Pérez-Segarra**
**Universitat Politècnica de Catalunya – Barcelona Tech (UPC), Heat and Mass Technological Center (CTTC)*
Terrassa, Barcelona, Spain, mail@cttc.upc.edu

*Christopher Hill**, Paolo Giangrande**, Shih Lai**, Giorgio Valente** and Sharmila Sumsurooah***
***University of Nottingham (UNOTT), Power Electronics, Machines and Control Group*
Nottingham, NG7 2RD, United Kingdom, c.hill@nottingham.ac.uk

Abstract

A flexible numerical platform based on libraries has been developed within the Dymola/Modelica framework to simulate Environmental Control Systems (ECS). The goal was to build up a flexible tool to analyse complex systems including their thermal and electrical perimeters at both steady and transient conditions focusing on three key characteristics: numerical robustness, optimal time consumption, and high accuracy. This document aims to underline both the most relevant features of the numerical tool and the main challenges addressed during its development. Some illustrative simulations are shown in order to highlight the tool capabilities.

1. Introduction

The interest of the European aeronautical industry in the development of more efficient and environmentally friendly aircrafts is at the core of the CleanSky2 European research program. Among the most promising actions to reduce the aircraft CO_2 footprint the implementation of the More Electric Aircraft (MEA) concept stands out. This approach considers a significant reduction - or complete elimination - of bleed air from the engines in order to reduce the fuel consumption and to enhance the aircraft overall energy efficiency. The aim is to free the engines from producing compressed air for secondary needs such as the Environmental Control System (ECS) and to supply the energy demand in form of electricity. In this sense new ECS configurations based on more complex interactions with the electrical system are necessary (electrical ECS or e-ECS). Both the ECS optimal design and its efficient operation are critical to attain the expected global efficiency improvements as, after propulsion, the ECS is the largest energy consumer in relatively large aircrafts.

The analysis of an e-ECS based on numerical simulations is particularly complex due to the large number of subsystems involved and their different physical phenomena, namely, thermal, electrical, pneumatic and mechanical. The extended thermal perimeter in e-ECS comprises new components and units (e.g. dedicated compressors for air pressurization, embedded Vapor Compression System (VCS)) and experiences important interactions with the electrical system (e.g. electrical drive systems, cooling of power electronic modules). The development of an updated system-oriented simulation platform to deal with the e-ECS complexity is crucial to cover the optimal design process not only from a thermodynamic engineer perspective (steady-state) but also from the control engineer point of view (transient behaviour).

The present work derives from a project within the CleanSky2 European research program whose aim is to develop a complete set of Dymola/Modelica libraries to simulate full e-ECS with the following requirements: high accuracy (numerical predictions close to correct values), robustness (numerical reliability within a wide range of operating conditions), and minimized computational time (to guarantee reasonable computational time of large architectures). The work conducted during the aforementioned project, regarding both the main thermal and electrical systems, is

DOI: 10.13009/EUCASS2019-767

summarized herein. The most significant contributions achieved within the project are emphasized (e.g. robust and efficient VCS simulation, enhanced heat exchanger treatment covering steady-state accuracy with transient behaviour, multilevel ATRU modelling, VCS compressor motor cooling, thermo-electrical linking, etc.). The strategies used as well as the numerical difficulties faced during the modeling of particular ECS components and subsystems are commented in the following sections. In addition, steady-state and transient simulation results are presented to illustrate the model capabilities.

2. Global architecture

The e-ECS configuration studied in the present work is briefly described in this section. The simplified scheme of the e-ECS thermal perimeter is shown in Figure 1 where the most relevant circuits are depicted.

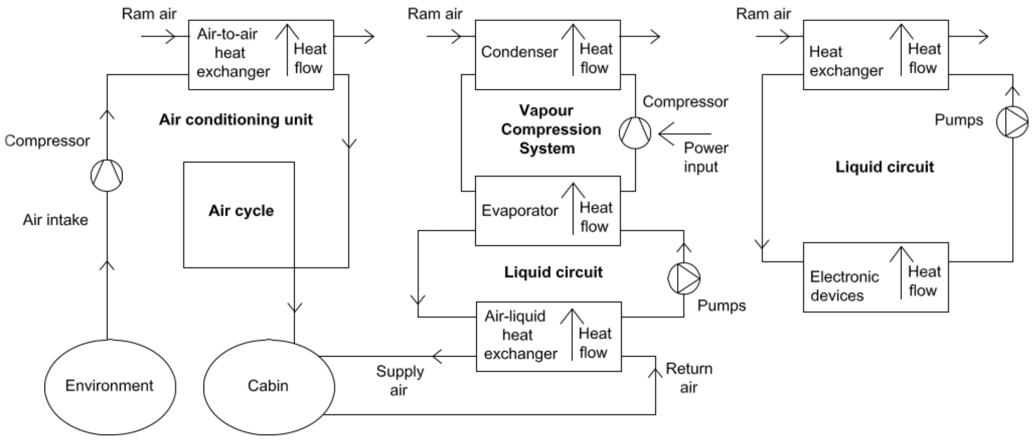

Figure 1: ECS schematic layout of thermal perimeter

The ECS is normally based on an air conditioning unit (ACU) that provides pressurized air at appropriate conditions of temperature and humidity to the cabin. The air is initially pressurized by means of dedicated compressors which are electrically driven and controlled while further adjustments of pressure, temperature and humidity are conducted throughout the air cycle. The ECS also includes a Vapour Compression System (VCS) to deliver additional cooling power when the ACU cannot cope with the cooling demand. The VCS is indirectly linked to the cabin by means of an additional liquid circuit and its role is to remove heat from the cabin and expel it into the environment. An additional liquid circuit drains heat towards the environment to cool down power electronic modules. These thermal systems are interrelated as they experience many direct and indirect interactions between each other via heat exchangers.

The fluid flow through thermal units is driven by turbo machines such as compressors, pumps or fans which in turn are powered and controlled by means of electrical drive systems. This thermo-electrical coupling goes beyond the mechanical transfer of energy as the main components of electrical drive systems are in turn refrigerated by the thermal units. The full set of thermal systems is also electrically controlled through other minor components such as valves.

3. Main components

The ECS is made up of a very large amount of components from both the thermal units (e.g. compressors, pumps, fans, turbines, heat exchangers, valves, tubes, reservoirs etc.) and the electric units (e.g. ATRU, inverters, motors, etc.). The primary goal for simulating such components was to provide low time consuming models to prevent from having bottlenecks during the global numerical resolution (most components are based on simplified mathematical formulations and fed with performance maps). The present section is devoted to introduce the modelling and characteristics of the most relevant components developed for the e-ECS libraries.

DOI: 10.13009/EUCASS2019-767

3.1 Turbo machinery

The vapour compression system and the main air conditioning unit are driven by compressors (fans are also used in the ram air circuit) while the liquid cooling circuits are driven by centrifugal pumps. The calculations are carried out from simple governing equations fed with empirical information given as performance maps, curves or constant values. The dynamics of the compression itself are not considered in the models in order to keep the component simulation time as low as possible. The aforementioned assumption is acceptable as the time constant for the compression process is significantly lower compared to the whole system global thermal and fluid-dynamic time constant. Nevertheless, the dynamics related to the accumulation of refrigerant inside such components are taken into account by means of a volume component connected in series.

3.2 Heat exchangers

Heat exchangers are probably the most challenging components of the whole system due to the complex phenomena involved. The studied ECS contains a wide variety of heat exchangers with different geometries and combinations of fluids such as refrigerants (vapour compression systems), water-glycol mixtures (liquid cooling systems), and air flows (air conditioning unit and ram air flow). In the present work a generic heat exchanger numerical structure has been implemented in order to flexibly model any particular heat exchanger. The basic structure consists of two independent components to simulate fluid flows and linked through a specific component that stands for the solid interface between them (see Figure 2 left). Three fluid flow models were developed, namely, refrigerant flow, liquid flow, and moist air flow, focusing on achieving the best compromise between calculation time and capacity to represent the physical phenomena.

Liquid flow model. The heat transfer prediction between the liquid flow and the solid interface is carried out considering a single control volume. The method implemented is based on an ε-NTU approach in order to optimize the calculation speed and also to prevent the calculation of unreal temperature values. The sensible heat between the fluid and the solid is calculated from their temperatures as follows:

$$\dot{Q}_s = \varepsilon C (T_{solid} - T_{fluid,in}) \quad \textbf{(1)}$$

Refrigerant flow model. The refrigerant model implemented herein is based on the switching moving boundary approach SMB [1] as it has low computational time (only three control volumes are used) unlike the traditional fixed volumes approach (where a large number of control volumes are needed). However, SMB models possess added numerical complexity not only because a mean void fraction has to be calculated but also because volumes have variable lengths and may be activated or deactivated. The successful implementation of the SMB model was the outcome of an extensive programming and verification effort. The flow domain scheme for an evaporator is depicted in Figure 2 (right) where three different zones are distinguished: sub-cooled, two-phase, and super heating. The conservation equations of mass and energy are calculated at each zone. Depending on the current flow conditions, the model switches between different operating modes so that zones are activated or deactivated as shown in Figure 3 (left).

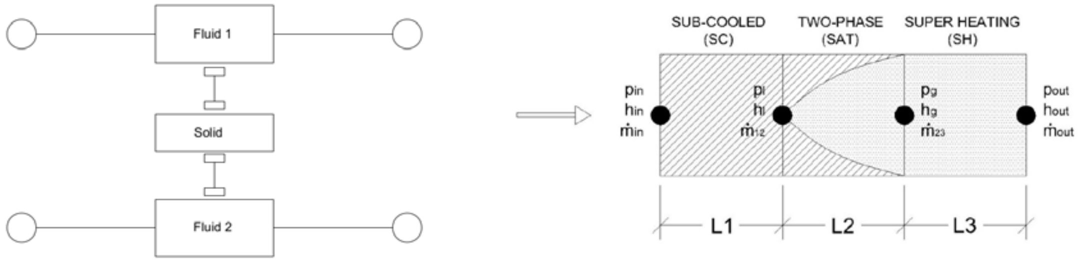

Figure 2: Heat exchanger basic structure (left) and evaporator SMB approach scheme (right).

The switching between modes (activation or deactivation of zones) leads to major modifications of conservative equations at each individual control volume. During transitions some local boundary values are rearranged and some equations are fully replaced. This procedure is necessary to retain the equations structure solved by Modelica. The switching criteria between modes has been carefully addressed. A zone is deactivated whenever its length becomes

DOI: 10.13009/EUCASS2019-767

smaller than a reference minimum length value, and on the contrary, a zone is activated whenever its local outlet enthalpy crosses any boundary saturation enthalpy value.

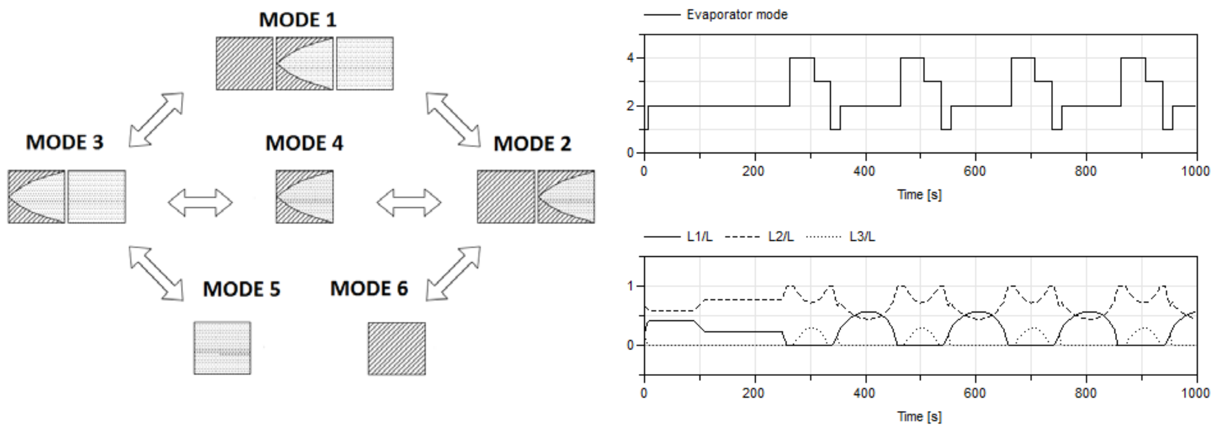

Figure 3: SMB evaporator model and transitions scheme (left) and robustness test result (right)

The SMB numerical stability has been extensively tested at all possible transitions and operating modes. For instance, Figure 3 (right) depicts the evolution of the zone lengths for a particular robustness test conducted on an evaporator. In this case the inlet specific enthalpies of both fluids were modified independently over time in order to force the heat exchanger to switch between modes 1, 2, 3 and 4 as the sub-cooled and the superheated zones were activated or deactivated (the CPU time to run this particular case was about 1 second). The pressure drop throughout the domain is calculated following an approach based on the assumption that the variation is linear.

Moist air flow model. The dry air flow calculation is conducted in a similar way to the liquid case presented in section 3.2.1. However, when moist air is considered the heat transfer due to water condensation should be also considered. The total heat transferred by the fluid is now calculated from both its sensible and latent terms:

$$\dot{Q} = \dot{Q}_s + \dot{Q}_l \quad (2)$$

$$\dot{Q}_l = \dot{m}_{air} \Delta_{hfg} (w_{out} - w_{in}) \quad (3)$$

The sensible heat term is calculated as in Equation 1, while the humidity at the exit is expressed as follows:

$$w_{out} = w_{solid} + (w_{in} - w_{solid}) e^{(-A\beta / \dot{m}_{air})} \quad (4)$$

3.3 Electrical components

ATRU. This section describes the models developed for the 12 pulse Autotransformer Rectifier Unit (ATRU). The input of the ATRU is connected to a three phase power supply and it outputs DC voltage to the inverter and PMSM machine. The ATRU is modelled in the ABC frame as well as in the DQ frame. Within the ABC frame, the ATRU is modelled as ATU and the RU separately and then the two models are combined to make the ATRU. Each of the aforementioned ATU and RU are modelled into further levels of complexity, which include the functional and behavioural models.

- **The functional models** are built using analytical equations of the circuits. They have fast simulation speed with respect to the behavioural model. The functional model of the ATU is based on analytical equations relating the output current and voltage of the two sets of secondary windings to the input current and voltage of the primary winding of the ATU [2]. The transformation ratio of the ATU is an important element of the modelling. The functional model of the three phase diode bridge Rectifier Unit (RU) is also based on analytical equations. The functional model of the ATRU is built by connecting the functional model of the Autotransformer Unit (ATU) model to the functional models of two Rectifier Units (RUs).

DOI: 10.13009/EUCASS2019-767

- **The behavioural models** are generated by using advanced component models from the Modelica library. They show the dynamics of the system but have slower simulation speed. The behavioural model of the 12 pulse ATU is built using the electromagnetic converter model of the Modelica library to represent the electromagnetic energy conversion between the three primary windings and the six secondary windings of the ATU. The three limbs of the core of the ATU are each modelled by using the generic flux tube with ferromagnetic hysteresis based on the Tellinen model and the Everett function [3]. The ATU model specifically uses the material M330-50A. The behavioural model of the three phase diode bridge RU is built by connecting ideal diodes from the Modelica library. The behavioural model of the ATRU is built by connecting the ATU model to two RUs.

The power losses that are computed in the ATU models include the secondary and primary copper losses as well as the hysteresis and eddy core losses. The power losses in the diode rectifier units consist of the diode losses. The total power loss of the ATRU, which is the sum of the power losses in the ATU and RU models, is extracted to the heat ports.

Inverter. There are many different approaches provided for modelling the power inverter which are switching ABC, non-switching ABC, and non-switching DQ. The switching ABC model provides the most similar waveform to the practical inverter. It uses the IGBT/MOSFET device in the switching, which shows the static and behavioural characteristics of the devices. However, using this model will cause a significantly high simulation time and computer loading. With the large system or large simulation time, it could crash the simulation due to out of memory. On the other hand, non-switching ABC model and non-switching DQ model do not show the static and behavioural characteristics of the devices, only the inverter power losses are calculated, based on the load voltage and current, which minimises the total simulation time. The aim of this inverter library is to measure the power inverter losses in the system.

- **Switching ABC.** In the ideal switching model, the switching device is modelled using the ideal switch and diode from Modelica library. Hence, only the conduction losses of the switch and diode are included in the inverter losses whereas the switching losses are neglected. In the switching IGBT model (see Figure 4), the ideal switches are replaced with a developed IGBT model, which includes both the conduction losses and switching losses. The behavioural characteristics are modelled with turn-on and turn-off energy losses. In addition, the power losses of the body diode are also included. In the switching MOSFET model, the conduction losses of the MOSFET are modelled as the on-resistance whereas the switching losses are modelled as turn-on and turn-off energy losses similar to the IGBT model. Furthermore, the model also includes the power losses of body diode.

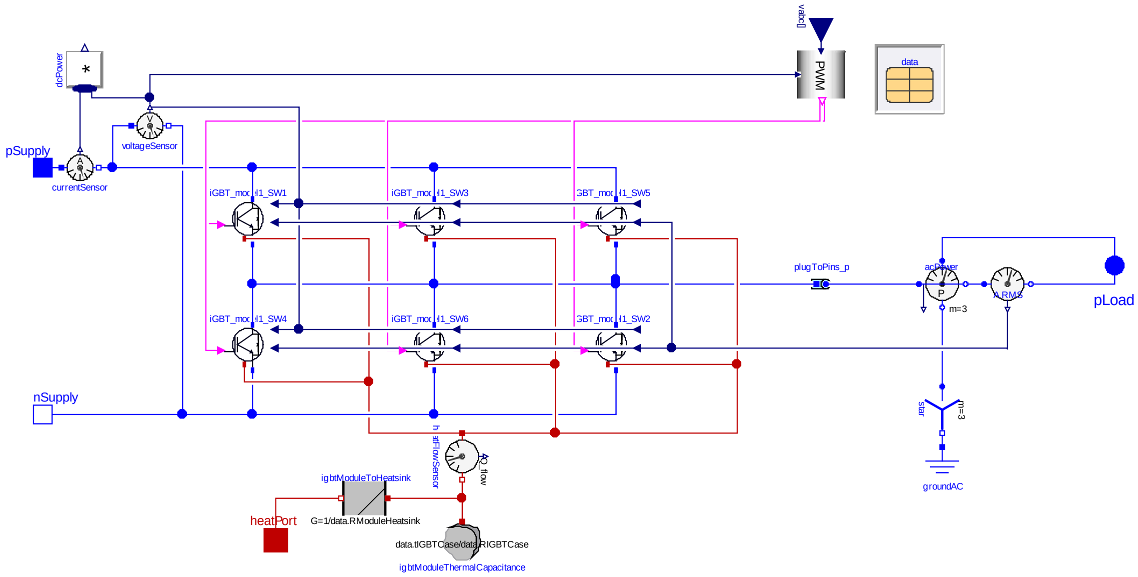

Figure 4: A diagram of inverter model for switching ABC model (Switching IGBT)

- **Switching ABC.** In this model, an analytical approach is implemented to calculate the power losses for a pulse width modulated inverter. The benefit of this model is the low CPU time. In big system or complex

DOI: 10.13009/EUCASS2019-767

systems, a key desired feature is low simulation time. The results of this model show significant reduction of simulation time over the switching ABC model. The concept of this model is to use the information from controller to approximate the current flowing in each switching device and diode. Hence, the conduction losses and switching losses can be approximated. The model is further classified into three sub-systems namely constant efficiency based losses, variable efficiency based losses and datasheet based losses.

- **Non-Switching DQ.** This model, it is similar to 'Non-Switching ABC' but the equations are performed in DQ domain. This leads to faster simulation time (CPU time) as it does not require inverse Clarke transformation and inverse Park transformation in the machine, controller and inverter side. In addition, the DQ domain does not depend on the tolerance of simulation time-step, which means that it can further minimise the simulation time. The model is further classified into three sub-systems same as 'Non-Switching ABC' namely constant efficiency based losses, variable efficiency based losses and datasheet based losses.

Machine. This paragraph presents the model description of a three-phase permanent magnet synchronous machine (PMSM) with permanent magnets placed on the rotor surface (surface mounted, i.e.: inductance $L = L_d = L_q$). The three-phase winding is assumed star connected with floating neutral point. Hence, parameters such as winding resistance and inductance are intended as line-to-neutral values. The Electrical Machine model includes the following two models:

- Permanent Magnet ABC. This Electrical Machine model is fed by phase quantities (v_a, v_b, v_c, i_a, i_b and i_c) and the Park's transformation is applied in order to compute the voltage and current quantities in the rotor synchronous reference frame. The voltage equations are then implemented in the rotor synchronous reference frame.

- Permanent Magnet DQ. This Electrical Machine model is fed directly by voltage and current quantities in the rotor synchronous reference frame and the voltage equations are implemented in the rotor synchronous reference frame.

Both the Permanent Magnet ABC and DQ models are then divided into three complexity levels:

- **Level 1.** In this Level only copper and mechanical losses are considered. A thermal network is included in order to perform steady state thermal analysis. The thermal model works under the assumption that all the machine losses are applied inside the slot and transferred to the coolant.

- **Level 2.** In this Level the considered losses are: copper losses, iron losses and mechanical losses. A thermal network is included in order to perform steady state thermal analysis. The thermal model works under the assumption that all the machine losses are applied inside the slot and transferred to the coolant.

- **Level 3.** In this Level all the losses are considered including: copper losses, iron losses, PM losses, mechanical and sleeve losses. A thermal network is included in order to perform transient thermal analysis.

4. Systems

This section is devoted to introduce the main aspects tackled to simulate the e-ECS constitutive systems, namely, the ACU, the VCS, the LCU, and the electrical drive systems focusing on achieving robustness and minimum computational time. The numerical issues addressed when combining multiple thermal systems and conducting the thermo-electrical coupling are also presented.

4.1 Vapour compression system

A vapour compression system is located at the core of the ECS described in Section 2. This unit is made up of several major elements, namely, a centrifugal compressor (to propel the refrigerant flow), a refrigerant-to-air condenser (to eject heat towards the environment), a refrigerant-to-liquid evaporator (to extract heat from the liquid circuit), and some additional minor elements as shown in Figure 5 (left). The main role of the VCS used in the studied ECS layout is to give additional cooling power to the air conditioning unit when needed (e.g. when relatively

DOI: 10.13009/EUCASS2019-767

high environment temperatures are considered). The VCS is a crucial part of the whole ECS and it is arguably the most difficult to tackle from both the physical phenomena and the numerical resolution point of views.

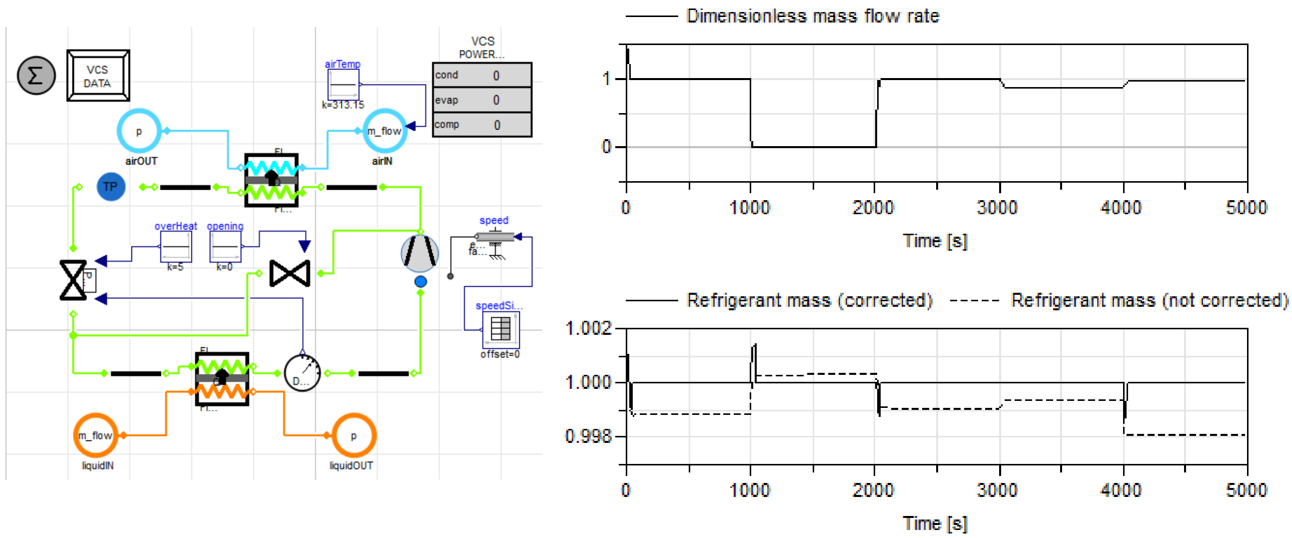

Figure 5: VCS scheme (left) and illustrative transient results (right)

The main numerical difficulties that have been addressed during the assembly of the VCS components and its modelling under the Dymola/Modelica framework are described in the following list. It is worth mentioning that all these aspects were tackled in the present work focusing on achieving robustness and minimum computational time.

- **Initialization.** The resolution of a system at time equal to zero is a critical numerical task as no information on the previous time step is available (appropriate initial values could be difficult to obtain specially for closed systems such as the VCS). The initialization goal is to assign consistent initial values for all variables and derivatives but also to provide suitable initial constraints to the equations. In this sense, a global component dedicated to this particular purpose has been developed in order to automatically set the initial values of all variables. Moreover, to enhance the resolution of components during the initialization both homotopy transformations and dynamic relaxation of certain variables were implemented.

- **Steady-state resolution.** A direct calculation of the initial steady-state cannot be achieved by setting all derivatives equal to zero because it leads to a singularity. This difficulty was addressed by reaching the steady-state by means of a meaningless transient relaxation starting from a set of guessed initial values.

- **Start-up/shut-down operations.** The system simulation at (near) zero mass flow rates is a considerable numerical challenge. At such conditions the solver time step is significantly reduced due to undesirable oscillations created by fast dynamics. To deal with these unwanted conditions the VCS components equations were rearranged to avoid any possible division by zero and all pressure drop equations were regularized to prevent steep pressure changes from occurring.

- **Refrigerant charge management.** The refrigerant mass amount conservation is another critical aspect to consider in VCS. The charge amount set at the simulation beginning can experience non-negligible variations during the simulation execution as long as the mass conservation undergoes small deviations in time due to the lumped nature of the two-phase flow heat exchanger models. The approach used in the present model consists in adjusting the refrigerant mass amount whenever its value deviates too much from the reference value by artificially injecting or extracting tiny amounts of mass into or from the circuit, respectively. Figure 5 (bottom-right) shows the total refrigerant amount throughout a particular transient simulation with and without applying the correction.

- **Transient resolution.** The system transient response throughout time can produce numerical issues when extreme modifications of the boundary conditions occur. The model has been tested at these conditions to assure robustness.

DOI: 10.13009/EUCASS2019-767

- **Thermostatic valve operation.** The VCS superheating is controlled by means of a thermostatic valve located between the condenser and the evaporator. This type of self-controlling systems can generate several numerical instabilities. The proposed approach consisted in using an adjustable valve combined with a PID controller that compares the reference superheating value with the measured one (PID parameters are adjusted from experimental data).

- **Phase changes.** The refrigerant running along this unit experiences phase changes inside both the evaporator and the condenser. This particular and complex phenomenon has been carefully tackled during the development of the heat exchangers (see Section 3.2).

The simulation results of an individual transient simulation of the VCS are shown in Figure 5 (right). The system has been studied for a period of 5000 seconds (considering 1000 intervals) and has been subjected to multiple events: compressor shut-down (at 1000 s), compressor start-up (at 2000 s), compressor speed reduction (-5% of reference value), and opening of by-pass valve (at 4000 s). The evolution of both the refrigerant mass flow rate and the refrigerant total mass are depicted in their dimensionless form in the top-right and bottom-right figures respectively. The CPU time for this particular transient simulation was less than 15 seconds. The CPU time needed for a steady-state simulation of the same system lies between 2 and 3 seconds. The specifications of the PC used to run all cases presented herein are: Intel(R) Core (TM) i5-2540M CPU @ 2.60GHz with 8192MB RAM.

4.2 Liquid cooling units

The ECS presented in Section 2 includes two independent liquid circuits. The main role of these units is to cool down either electric devices (by directly draining heat into ram air) or the aircraft cabin (by indirectly draining heat towards the VCS). In these units the fluid is driven by one or more pumps which could be connected in series or parallel configurations. They also include heat exchangers where heat is either extracted or ejected and other minor elements such as valves, ducts and reservoirs to enable fluid expansion. Figure 6 (left) depicts a liquid circuit scheme with both heat exchangers and pumps placed in parallel.

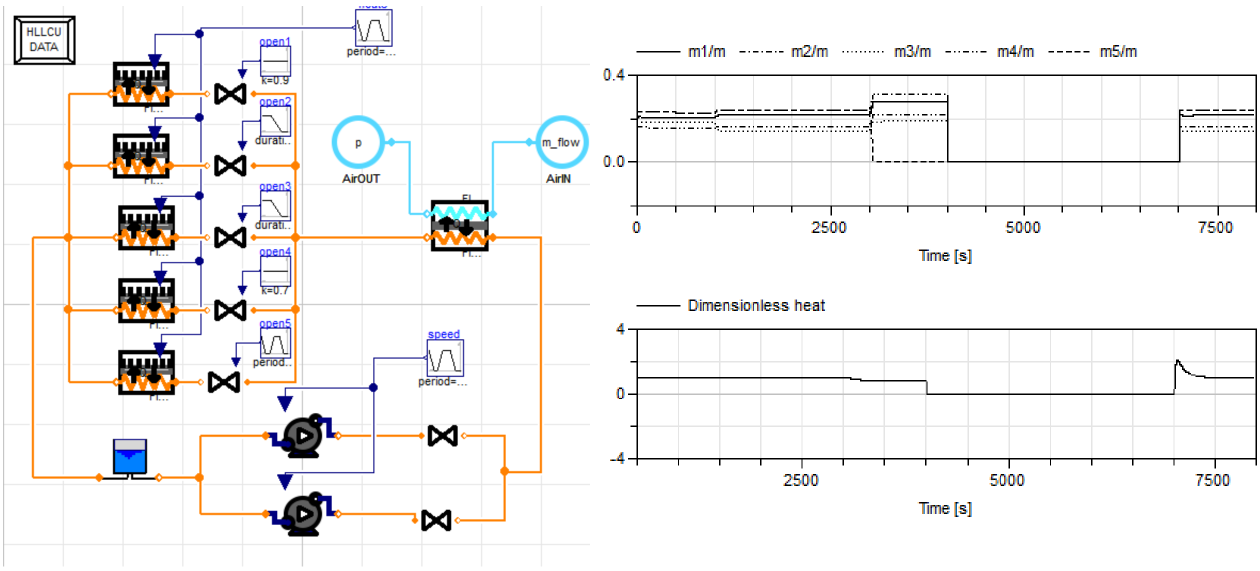

Figure 6: LCU illustrative scheme (left) and transient results (right)

During the assembly of the LCU components similar numerical difficulties to those of the VCS have been faced, namely, the initialization, the steady and transient resolutions, and the start-up/shut-down operations. However, some additional issues have been tackled for these particular units.

- **Layout variability.** The library developed to simulate liquid loop circuits was flexible enough to model different liquid cooling circuit configurations with distinct components and roles (The ECS studied herein included two different liquid cooling loops).

DOI: 10.13009/EUCASS2019-767

- **Fluid expansion.** The handling of fluid expansion is a critical aspect in liquid loops where pseudo-incompressible fluids are used. In this sense the appropriate modelling of a reservoir and its link to the circuit must be carefully addressed.

- **Parallel circuitry.** The need for flow branching at several parts of the circuit is a challenging task from the simulation point of view (the solver faces additional stress as flow distribution complexity increases). The pressure drop equations of all the components involved must be appropriately defined in order to prevent the solver from failing.

An illustrative transient simulation of the particular circuit presented in Figure 6 (left) is depicted in Figure 6 (right). In this particular test a transient simulation to test the flow distribution through parallel branches has been conducted (period 8000 seconds with 4000 intervals). The flow through each parallel branch containing a heat exchanger has been modified during the simulation by closing or opening its corresponding valve as follows: valve number 3 opening degree reduced 20% (at 1000 s), valve number 5 fully closed (at 3000 s), pumps are turned off (at 4000 s), valve number 5 fully opened (at 5000 s) and finally pumps are turned on again (at 7000 s). The evolution of the mass flow rate through each heat exchanger together with the total heat removed are plotted in the top and bottom of Figure 6 (right) respectively. The CPU time for this particular simulation was about 72 seconds. The CPU time needed for a steady-state simulation of the same system lies between 4 and 5 seconds.

4.3 Air circuits

The air conditioning circuit role is to provide suitable pressure, temperature and humidity to the cabin air. In the ECS configuration studied herein the compressed air is obtained by means of dedicated compressors unlike systems where the compressed air is directly provided by the engines. Besides the compressors, the air conditioning unit contains several air-to-air heat exchangers, a turbine, and other minor components such as valves, water sprays/extractors and so on. A part of this unit scheme is shown in Figure 7 (left). It is worth mentioning that an additional ram air circuit to drain the whole ECS unit heat (not shown in this document) has also been modelled.

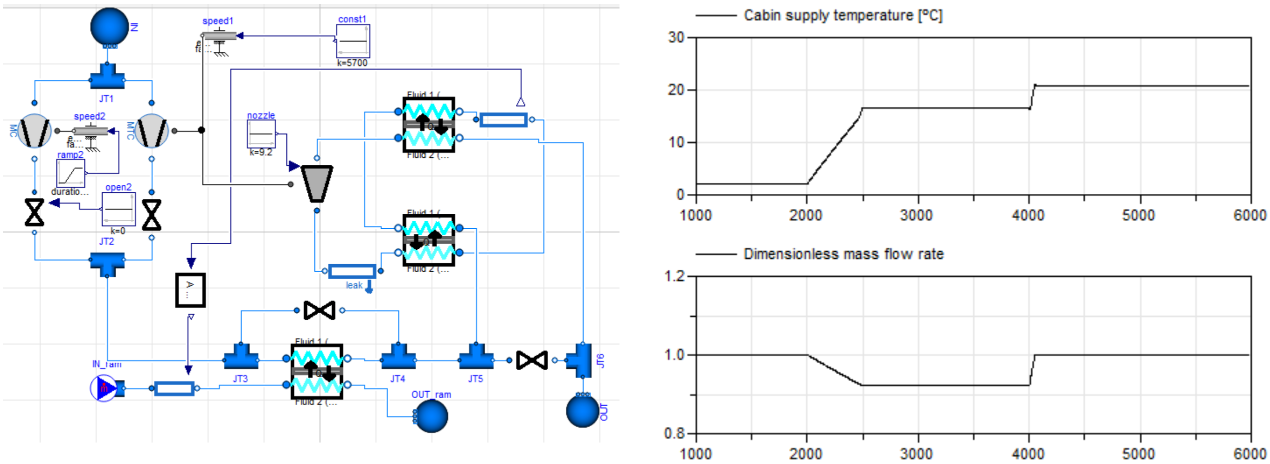

Figure 7: Air conditioning unit illustrative scheme (left) and transient results (right)

In general, the simulation of ACU units presents less numerical difficulties compared to the other units as the fluid is not flowing through a closed loop (the incoming air is given as a boundary condition obtained from the airplane external atmosphere conditions). Nevertheless, some particularities make this unit also challenging to model appropriately:

- **Moist air.** The management of the liquid water content together with the humidity of the flowing air is very important to accurately predict the heat transfer phenomena occurring through heat exchangers. Three different air-to-air heat exchangers have been developed for this unit where both water condensation and evaporation has been considered.

- **Turbo machines.** The simulation of this unit has to deal with challenging configurations of turbo machines, namely, centrifugal compressors working in parallel and a turbine transferring work to one of the compressors.

DOI: 10.13009/EUCASS2019-767

An illustrative transient simulation of the particular circuit presented in Figure 7 (left) is depicted in Figure 7 (right). The simulated period was 6000 seconds while the number of intervals considered was 3000. The main goal of this simulation was to observe the unit response to changes on the environmental temperature and adjustments to the compressor speed. Two simulation events were considered: progressive ambient temperature increase from 30 to 50 ºC (starting at 2000 s and finishing at 2500 s) and compressor speed increase of 10 % (at 4000 s). The CPU time for this particular simulation was 4 seconds. The CPU time needed for a steady-state simulation of the same system lies between 2 and 3 seconds.

4.4 Electrical drive system

The model of the overall electrical drive system is represented in the block diagrams of Figure 8 a) and b) which show the model schematics in the ABC and DQ reference frames, respectively. The presented schematics have been implemented in the Dymola/Modelica environment. The main difference between these two reference frames is that AC voltages and currents which are sinusoidal, and hence time varying, in the ABC frame become constant values in the DQ frame. Computationally this decreases simulation times significantly.

An overview of overall electrical drive system will be presented hereafter. Taking as example the ABC model, it is possible to distinguish the four main sub-components: electrical grid, Autotransformer Rectifier Unit (ATRU), inverter, controller and electrical machine. The drive system role is to power the compressor of the VCS presented in Section 4.1. The compressor rotational speed needs to be regulated by the electrical machine, therefore a controller unit is introduced for this purpose. Indeed, the speed regulation is implemented in the controller unit together with current regulation. Proportional Integral Derivative (PID) regulators are employed as controllers. An electrical grid has been created in order to provide electrical power to the drive system.

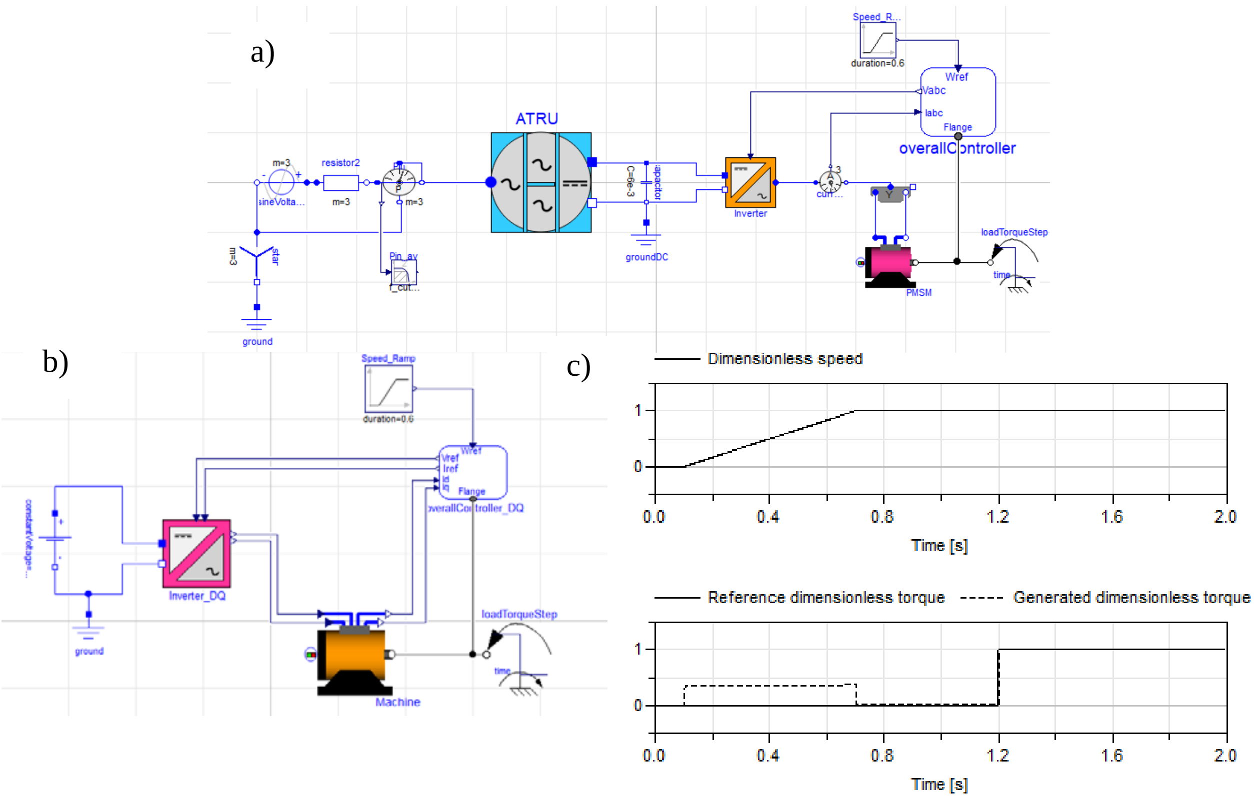

Figure 8: Electrical drive system: a) ABC model; b) DQ model; c) illustrative transient results (rotational speed and generated torque of the electrical machine)

Figure 8 c) shows an illustrative result of the drive system operation. A speed ramp is applied as reference so that the electrical machine accelerates reaching the rated speed in about 0.6 s (see top of Figure 8c)). It can be observed from the bottom of Figure 8 c) that the torque generated by the machine is about 40% of the reference value during this time. At 1.2 s a load torque (i.e. from the compressor) is applied as a step, therefore the machine generated torque

DOI: 10.13009/EUCASS2019-767

increases in order to compensate the required torque demand. In the presented results the simulated time is set equal to 2 seconds. The CPU times are 0.9 and 0.303 seconds when the ABC or DQ models are employed respectively. The latter model reduces the simulation time by a factor of three.

4.5 Thermo-electrical linking

The VCS refrigerant flow is driven by a centrifugal compressor which is powered and controlled by means of an electrical drive system (see sections 4.1 and 4.4). These two systems are connected mechanically and thermally. On the one hand, energy is transferred from the electric machine to the fluid, and on the other, heat is drained from the electric drive components to the fluid (The flow of refrigerant is diverted to pass through the electrical components and refrigerate them).

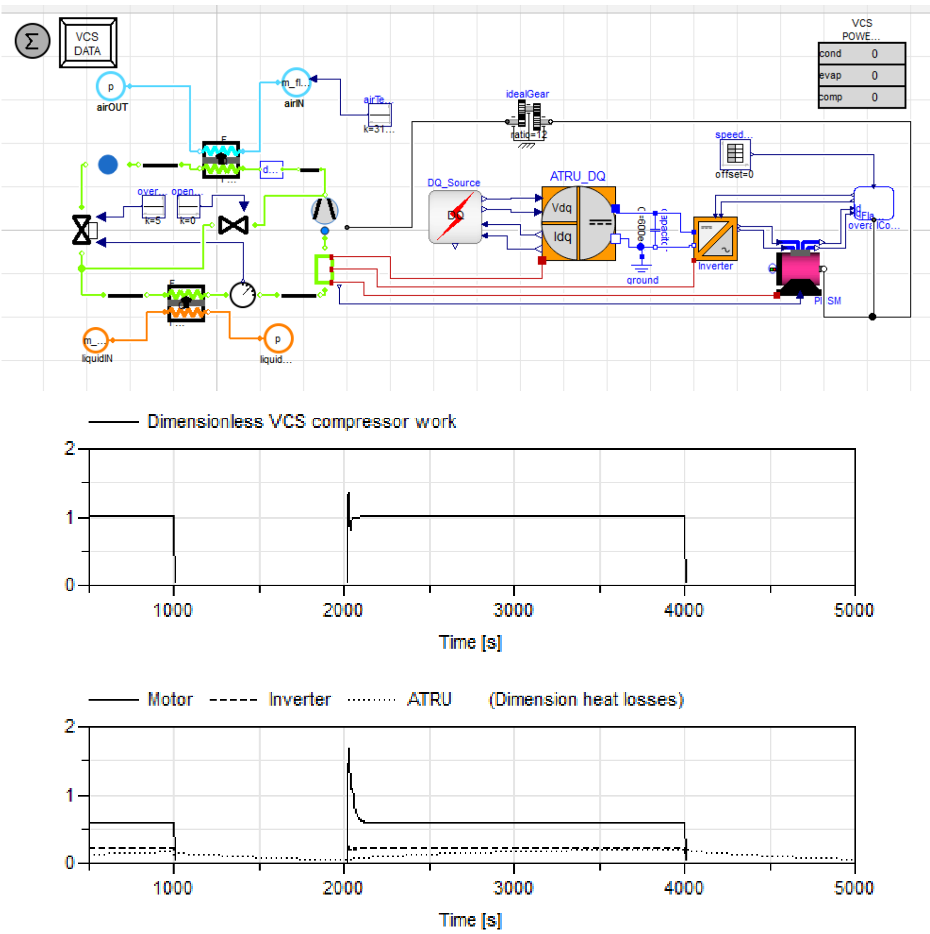

Figure 9: VCS and electrical drive system: scheme (top) transient simulation results (bottom)

The simulation of the VCS and the electrical drive system interactions deals with additional numerical difficulties besides the particular challenges of each individual system.

- **Multiple physics.** The joining of the two systems represents a challenge from the numerical point of view as not only thermal but also electrical and mechanical physics are involved. The solver time steps used for the resolution of each individual system can significantly differ from one another. Therefore, the combined system is forced to cope with the lower time step leading to increased global computational time. The approach used in the present project consisted in developing a fast model for the electrical components able to run under larger time steps.

- **Setting up connections.** The mechanical connections were modelled based on standard library components and presented no major issues. The thermal connections were achieved via standard connectors linking the three main electric drive system components (i.e. ATRU, inverter and machine) with a VCS component

DOI: 10.13009/EUCASS2019-767

specially dedicated for this purpose. The heat losses were calculated within the electrical system but based on the refrigerant flow conditions calculated in the VCS.

Figure 9 depicts illustrative transient results of a particular simulation subjected to the following events: compressor shut down (at 1000 s), compressor switched on (at 2000 s) and finally compressor shut down (at 4000 s). The full simulated time was 5000 seconds considering 1000 intervals. The evolution of both the dimensionless compressor work and the three different heat flows are presented. The CPU time for this particular transient simulation was about 62 seconds while the CPU time needed for a steady-state simulation of the same system is about 15 seconds.

4.6 Full thermal system

The full thermal perimeter schematically depicted in Figure 1 has been assembled combining the subsystems detailed in the previous sections. The main role of the studied system is to provide appropriate air conditions to the cabin by means of the ACU and, if necessary, the VCS support. The cooling of power electronics modules with the LCU has also been considered in the simulation. Although this latter system seems to be unrelated to the cabin air conditioning goal (see Figure 1) the resolution is carried out simultaneously as all the studied subsystems share the same ram air circuit where heat is drained. The different subsystems may influence each other as some heat exchangers are connected in series throughout the ram air system. The ram air circuit is not described in this work but has also been simulated.

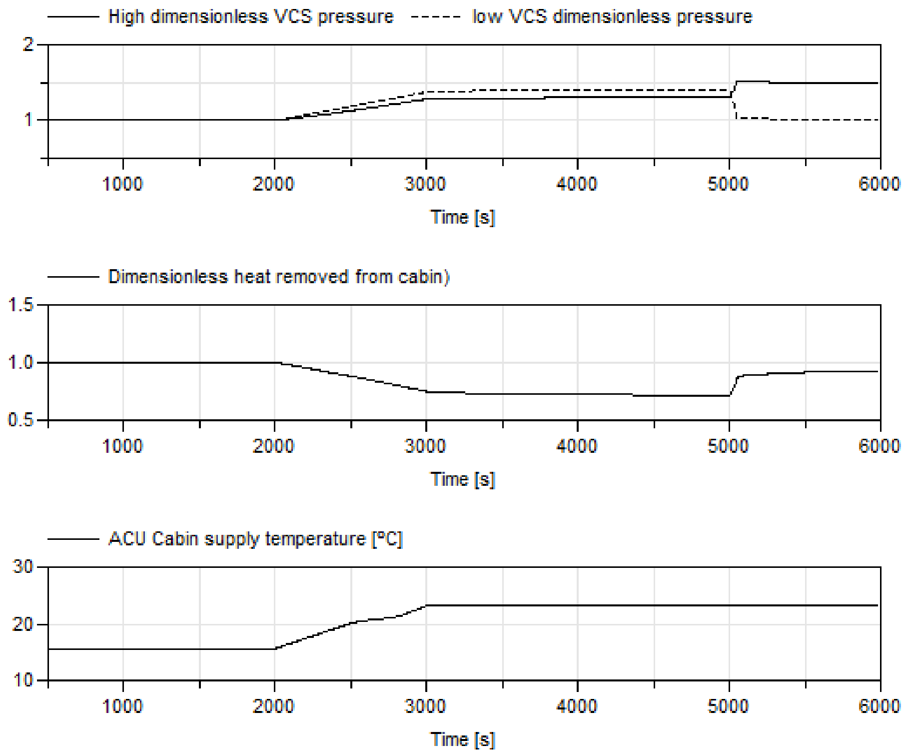

Figure 10: Complete ECS thermal perimeter transient results

New numerical challenges arise when two or more subsystems are directly connected and solved simultaneously. The following relevant aspects were addressed:

- **Complexity increased.** The number of components to be solved is drastically increased. The simulation of many subsystems, including several closed circuits with different fluids, must be carefully managed together with their interactions between them. The subsystems are usually connected through common components such as the evaporator which is shared by the VCS and the LCU.

- **Initialization.** The initialization must deal with all the aspects presented in section 4.1 but also with new difficulties. The solver experiences maximum stress when initializing a combination of systems. Finding appropriate initial values and initial constraints to equations is critical but using additional components to

DOI: 10.13009/EUCASS2019-767

assist the initialization is necessary (e.g. components to delay and/or relax the information transferred from one system to the other).

Results of a transient simulation of the full ECS thermal layout are plotted on Figure 10. The VCS high and low dimensionless pressures, the dimensionless heat removed from the cabin through the LCU, and the ACU cabin supply temperature are plotted. The simulation included the following sequence of events: ambient temperature linearly increased from 40 to 50 ºC (starting at 1000 s and finishing at 2000 s) and compressor rotating speed increased (at 5000 s). The simulation time was 6000 seconds with an interval of 1000. The CPU time for this particular simulation was 241 seconds. The CPU time needed for a steady-state simulation of the same system lies between 20 and 40 seconds.

5. Conclusions

A complete set of libraries to simulate e-ECS with extended thermal perimeter has been developed within the Dymola/Modelica framework. The simulation of an illustrative e-ECS configuration with different thermal and electrical subsystems has been achieved. A significant number of numerical difficulties were addressed during the development of the aforementioned libraries concerning both the components modelling and the systems resolution aspects. Some of the most important achievements are highlighted:

- **Component models.** Many models have been developed focusing on finding the best compromise between accuracy and calculation time consumption. Special attention has been addressed to heat exchangers and electrical models. On the one hand, a flexible heat exchanger model structure has been built up and complex phenomena such as phase change and air humidity management has been successfully tackled, on the other hand, electrical components were developed considering different complexity levels.

- **Subsystem models.** A wide variety of thermal systems working with different fluids (refrigerants, liquids and moist air) have been assembled and numerically tested. Many challenging difficulties have been addressed during the development of subsystems, namely, numerical initialization, start-up/shut-down simulations, zero mass flow rate conditions, closed circuits, components placed in parallel configurations, fluid charge management, reversed flow and others. An electrical drive system has also been developed combining its main components, namely, ATRU, inverter and machine, considering different complexity levels. The steady-state calculation time achieved for the thermal and electrical units was relatively low (just few seconds). Dynamic cases were also carried out in order to test the subsystem responses to control procedures.

- **System assemblies.** The developed thermal subsystems have been combined between them as well as with electrical subsystems in order to build up a complete e-ECS model. The thermo-electrical assemble has been studied focussing on the VCS thermal and mechanical connections with its corresponding electrical drive system. A full thermal ECS has been numerically analysed at steady and transient conditions. Several strategies were implemented in order to appropriately initialize and simulate such complex configurations.

Acknowledgements

This work has been developed within the EU H2020 Clean Sky 2 research project "Development of MODELICA Libraries for ECS and Thermal management architectures - MALET" (grant agreement Nº 686783).

References

[1] J.M. Jensen and H. Tummescheit, “Moving Boundary Models for Dynamic Simulations of Two-Phase Flows”, *in Proceedings of the 2nd international Modelica conference,* March 2002, Oberpfaffenhofen, Germany.
[2] Sewan Choi, Prasad N. Enjeti and Ira J. Pitel "Polyphase transformer arrangements with reduced kVA capacities for harmonic current reduction in rectifier-type utility surface" *IEEE Transactions on Power Electronics*, Vol. 11, No. 5, September 1996.
[3] Johannes Ziske, Thomas Bodrich, "Modelica models for magneric hysterisis materials and transformers", *in Proceedings of the 10th international Modelica conference,* March 2014, Lund, Sweden.